

RESPONSE OF SEISMIC ISOLATED ELEVATED BRIDGE DUE TO SLIGHTLY STRONG EARTHQUAKES IN 1995 AND 2018

Xiang YIN¹ and Yoshikazu TAKAHASHI²

¹Student member of JSCE, Graduate Student, Dept. of Civil Eng., Kyoto University
(Kyotodaigaku-Katsura, Nishikyo-ku, Kyoto, 615-8540, Japan)
E-mail: yin.xiang.48a@st.kyoto-u.ac.jp

²Member of JSCE, Dr. Eng., Professor, Dept. of Civil Eng., Kyoto University
(Kyotodaigaku-Katsura, Nishikyo-ku, Kyoto, 615-8540, Japan)
E-mail: takahashi.yoshikazu.4v@kyoto-u.ac.jp

This paper studies the behavior of seismic isolated structure (Pier 408 of Matsunohama Viaduct) under slightly strong earthquakes (M4.0-6.9) with seismic acceleration data recorded in the 1995 Kobe Earthquake and the 2018 Osaka Earthquake. The target structure was modeled by a 1DOF model with two parameters (stiffness and damping ratio) which are to be determined. The damping ratio is estimated using the Random Decrement Technique (RDT). Multiple numerical simulations are carried out with different preset stiffness to obtain the acceleration responses of the structure, which are later compared with observed results to calculate the RMS value. The model with minimum RMS value is considered to have stiffness closest to reality. Results show that the system identification technique works fine and the stiffness of the lead rubber bearings (LRBs) becomes larger in 23 years.

Key Words : 2018 Osaka Earthquake, 1995 Kobe Earthquake, seismic isolation, elevated bridge

1. INTRODUCTION

Japan is one of the countries located in earthquake prone regions and structures often become the victims of earthquakes. Many cases of structures collapse occurred when being exposed to past strong earthquakes. Owing to the collapse of structures, society suffered enormous costs and inconveniences. Meanwhile, elevated bridges are one of the most important parts in nowadays transportation networks, which are considered as the lifeline structures. Since they play an essential role in domestic transportation supporting the daily functions and needs, they also required higher seismic performance than standard structures. Aim to improve the seismic performance of structures during earthquakes, the number of the structures using seismic base isolated devices has an increasing tendency after past large-scale earthquakes such as 1995 Kobe Earthquake and 2011 Tohoku Earthquake. The number of earthquakes occurring in Japan in the average of one year is shown in Fig.1 and the calculation was based on the data collected from 2001 to 2011 by Japan Meteorological Agency. From this figure, we can see that

the large-scale earthquake (>M7.0) rarely occurs, however, the slightly strong earthquakes (M4.0~M6.9) frequently occurs.

Many researches^{1),2)} have been carried out on analyzing the behavior of seismic base isolated structures during large scale earthquakes. The predicted response of the isolators shows good identification results based on their numerical simulation models. In those models, LRBs were all modeled with a bilinear force-displacement relation. Previous studies³⁾ also stated that the real damping ratio and stiffness of the structure should be different to the setting equation in Design Manual of Bridge Bearing when small shear strain is smaller than 10%. In their study, the damping ratio tends to be decreased to zero and the stiffness is much larger than the Design Manual of Bridge Bearing setting stiffness when the shear strain is extremely small. However, few researches have been done on analyzing the response of seismic base isolated structure due to slightly strong earthquakes. Therefore, identify the modal parameters and clarify the behavior of seismic base isolated structures at actual slightly strong earthquake is necessary.

Previous studies⁴⁾ also pointed out that the stiff-

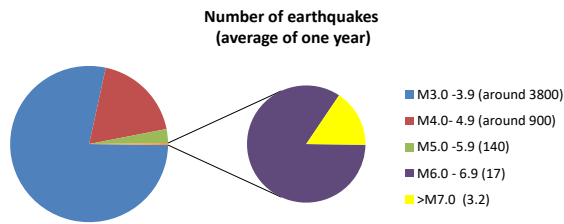


Fig.1 Number of earthquakes occurring in Japan in the average of one year.

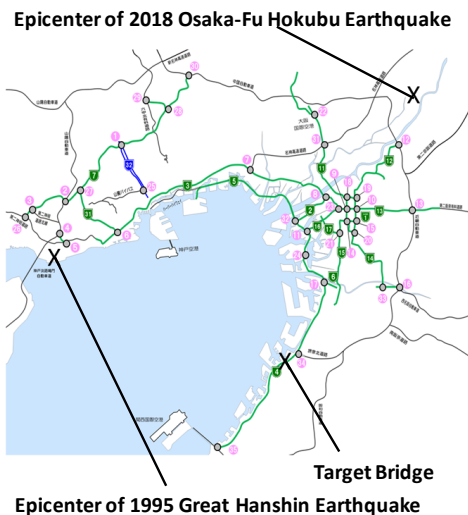


Fig.2 The location of the target structure.

ness of the LRBs will increase and the damping ratio tends to be decrease because of the aging of the LRBs. Therefore, checking whether stiffness and damping ratio change and how much they change are also important issues. For this purpose, system identification was performed by using the seismic acceleration recorded in both 1995 Kobe Earthquake and 2018 Osaka Earthquake for same target structure (Pier 408 of the Matsunohama Viaduct). Besides, Yoshida et al.⁵⁾ has also done research to evaluate the performance of Matsunohama Viaduct P408 during 1995 Kobe by the model of one degree of freedom system. This is the same target structure with this study. Therefore, we compare identification result with the previous identification result to justify feasibility and validity of the identification method.

The 2018 Osaka Earthquake is measured as Magnitude 6.1 with its epicenter (Latitude 36.1N, Longitude 139.9E) in the Takatsuki area of northeastern Osaka, at a depth of 13.2 kilometers. Shaking from the earthquake was felt strongly in the prefecture and the nearby areas such as Hyogo Prefecture and Kyoto Prefecture and it also had varying degrees of damage or effect to the structures around the epicenter. On the contrary, 1995 Kobe Earthquake struck the southern part of Hyogo Prefecture, Japan, including

the region known as Hanshin on January 17, 1995. It is measured 6.9 on the moment magnitude scale and had a maximum intensity of 7 on the JMA Seismic Intensity Scale. Its epicenter (Latitude 34.59°N, Longitude 135.07°E) was the northern part of Awaji Island in the Inland Sea, 20 km off the coast of the port city of Kobe. In addition, the earthquake resulted in more than 6,000 deaths and over 30,000 injuries and the economic loss as a result of this earthquake is estimated to reach \$200 billion. The objective structure, Pier 408 of the Matsunohama Viaduct is located 30 km away southwest from the 2018 Osaka Earthquake epicenter and 35km away southeast from the 1995 Kobe Earthquake epicenter as shown in Fig.2.⁶⁾ The results of responses cannot be achieved by conducting experiments due to its scale, feasibility and monetary issues. Therefore, a computer simulation based on commercial software OPENSEES is more realistic and feasible in this study.

2. TARGET BRIDGE DESCRIPTION

(1) Target bridge basics

The objective bridge, Matsunohama Viaduct is located on the Bay Shore route of Hanshin No. 5 Expressway in Izumiotsu Prefecture, 30 km away southwest from the 2018 Osaka Earthquake epicenter and 35km away southeast from the 1995 Kobe Earthquake epicenter and the seismic acceleration response has been recorded during the earthquake. Matsunohama Viaduct is one of the pioneer structures with special consideration for earthquake resistant design and lead rubber bearings (LRBs) are used to improve the seismic response of the viaduct. The target bridge was built in 1991 and a seismic reinforcing work was been done in November 1995, 10 months after the 1995 Kobe Earthquake. In order to record the seismic behavior of the structure better, acceleration recorder sensors that can obtain 400 seismic data has been installed into 22 positions. As shown in Fig.3, this four span continuous bridge has an overall length of 211.5 m. The two middle spans are 60 m, and the side spans are 46.5 and 45 m. The superstructure consists of two non-composite steel box girders and is supported by lead rubber bearings (LRBs) at the inner piers (P406 to P408) and on pivot roller bearings at the end piers (P405 and P409). Two side stoppers are installed with 5-mm clearance prevent movement in the transverse direction, so bearings can only move in the longitudinal direction. Reinforced concrete, single-column T shaped piers, founded in pile caps, are used for the substructure, and groups of the cast in place reinforced concrete piles of 1.2 m diameter are used for the foundation. Additionally, Pier P408 is instrumented with four seismometers for research at one meter underground,

footing, pier top and girder as shown in Fig.4. When the earthquake occurs, seismometers are able to record acceleration in the vertical, transverse and longitudinal direction of the bridges axis at a data-sampling rate of 100 Hz.

(2) Target bridge bearings

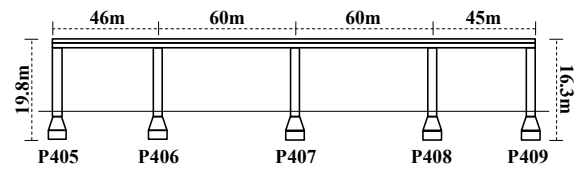
Lead rubber bearings (LRBs) have been installed between the pier top and girder in order to improve the seismic response of the viaduct. The plan view and elevation of the LRBs are shown in Fig.5. According to the experiment data from Hanshin Expressway, the loading test results when the shear strain is 4% and 70% are shown in Fig.6.⁷⁾ From the force-displacement relationship graph, we can pick up that the corresponding equivalent stiffness is 75460N/mm when the shear strain is 1.5% and 14210 N/mm when the shear strain is 70%. In this study, since the shear strain 1.5% is small enough, we define the corresponding stiffness as the experimental primary stiffness. Obviously, the primary stiffness according to the Design Manual for highway bridges bearings is larger than experimental primary stiffness since it represents the stiffness when the shear strain is around 80%. Besides, based on equation as shown in Eq. (1), the corresponding equivalent shear modulus can also be calculated based on its stiffness.

$$G(\gamma) = \frac{K_s \sum t_e}{A_e} \quad (1)$$

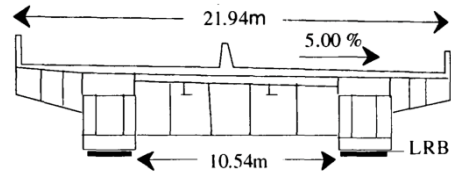
Base on the corresponding calculated shear modulus, the relationship between the shear strain and the equivalent shear modulus is simulated and plotted in Fig.7.

3. OBSERVATION RECORDS

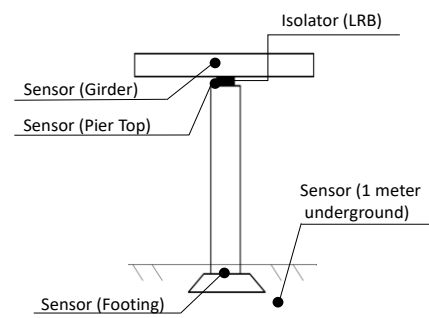
The maximum response acceleration of the target bridge are summarized in Table1. The acceleration record observed in longitude direction of 1995 Kobe Earthquake and 2018 Osaka Earthquake are shown in Fig.8 and Fig.9 respectively. Additionally, from the acceleration response spectrum in longitudinal direction shown in Fig.10, we can easily find out that the peak of footing appears at around 0.68 second cycle, the peak of pier top appears at around 0.18 second cycle and the peak of girder appears at around 0.69 second cycle in 1995 Kobe Earthquake. For the 2018 Osaka Earthquake condition, the peak of footing appears at around 0.38 second cycle, the peak of pier top appears at around 0.18 second cycle and the peak of girder appears at around 0.12 second cycle can be confirmed.



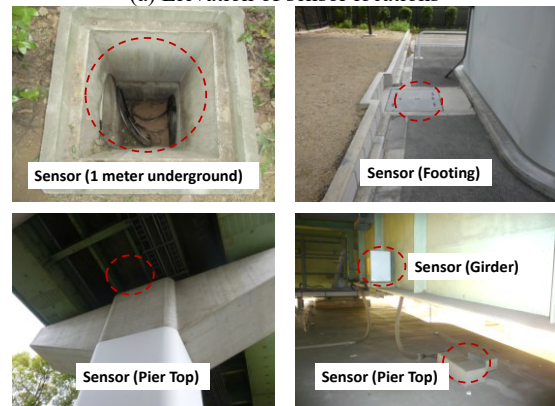
(a) Longitudinal Elevation of the bridge



(b) Cross Section of the superstructure
Fig. 3 Elevation and Cross Section.



(a) Elevation of sensor locations



(b) Location of sensors

Fig. 4 Location and Elevation of sensors.

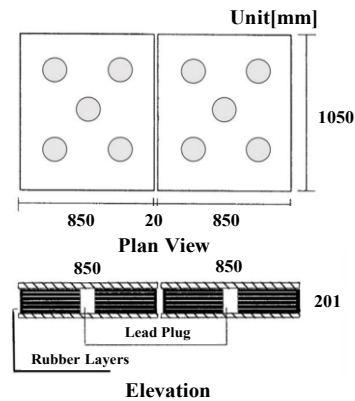
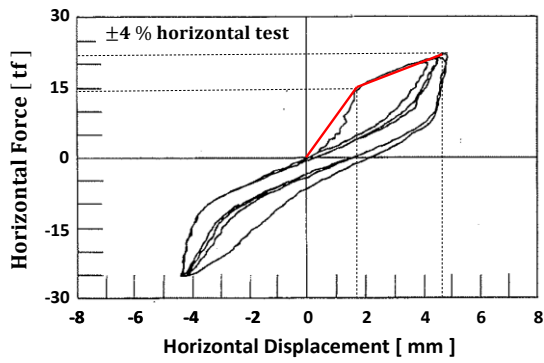
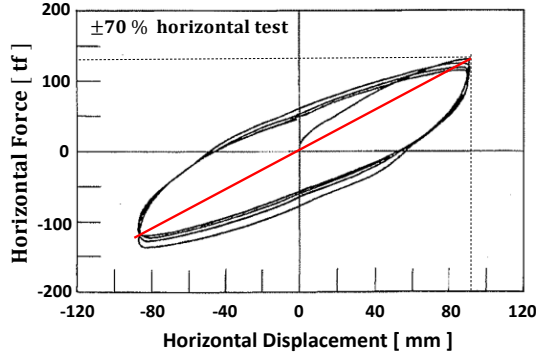


Fig. 5 The plan view and side view of LRBs.



(a) ±4 Horizontal Loading Test



(b) ±70 Horizontal Loading Test
Fig.6 Loading test result⁽²⁾.

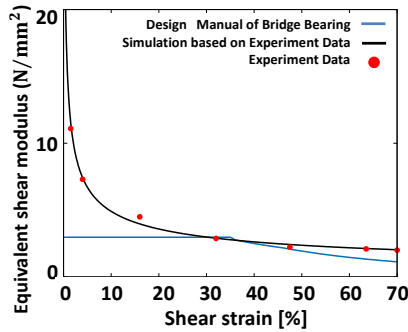


Fig.7 Relationship between shear strain and equivalent shear modulus.

Table1 Maximum response acceleration.

	1995 Kobe EQ	2018 Osaka EQ
Underground(-1m) Long.	144.6 gal	89.1 gal
Underground(-1m) Trans.	134.9 gal	150.1 gal
Underground(-1m) Vert.	115.6 gal	67.0 gal
Footing Long.	104.4 gal	128.7 gal
Footing Trans.	126.1 gal	65.2 gal
Footing Vert.	68.8 gal	58.0 gal
Pier Top Long.	200.8 gal	207.2 gal
Pier Top Trans.	356.8 gal	79.7 gal
Pier Top Vert.	76.5 gal	59.4 gal
Girder Long.	189.2 gal	227.8 gal

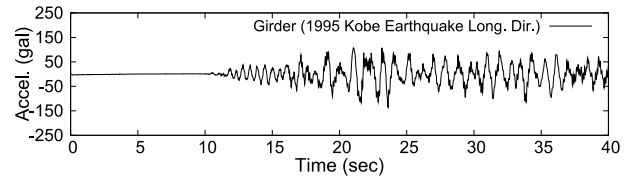
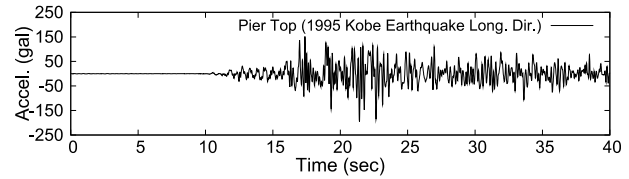
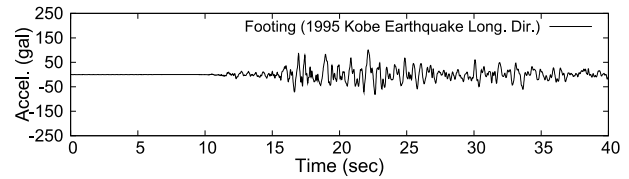
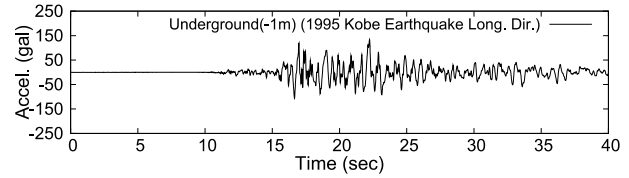


Fig.8 Acceleration observation record in 1995 Kobe Earthquake (05:46:59 17th January 1995).

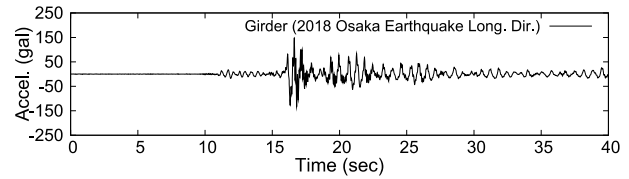
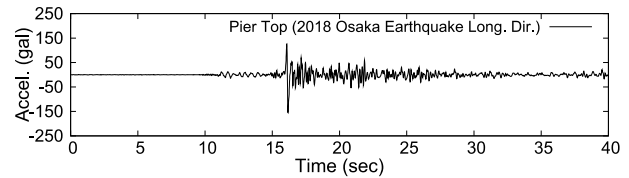
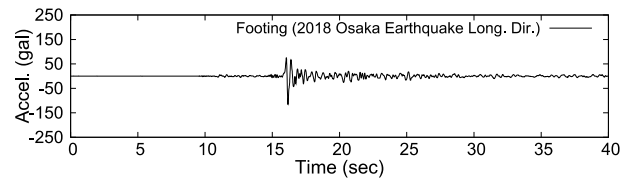
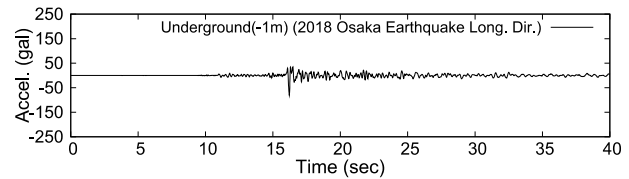


Fig.9 Acceleration observation record in 2018 Osaka Earthquake (07:58:43 18th June 2018).

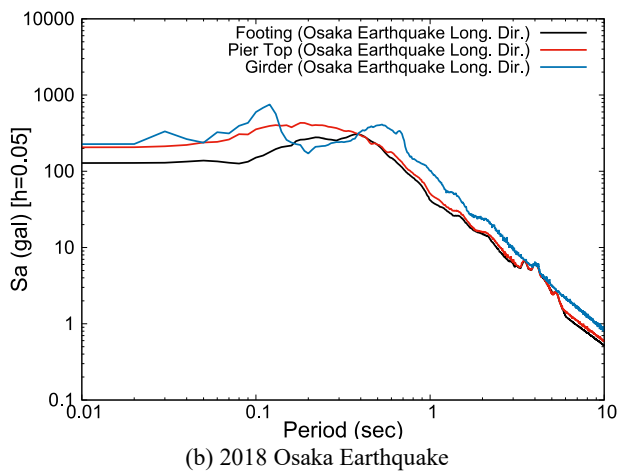
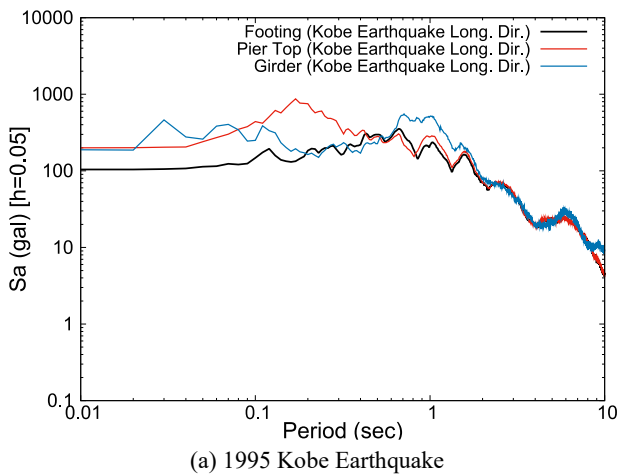


Fig. 10 Acceleration response spectrum in Long. Direction.

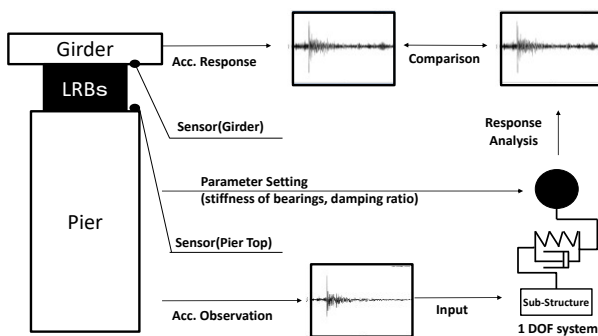


Fig.11 The outline of the identification method.

4. METHODOLOGY AND MODELLING

Fig.11 shows the outline of the identification method. When earthquake happens, the acceleration of the ground motion, substructure and the superstructure will be recorded. In this study, the block of Matsunohama Viaduct is separated into three parts, which are footing, pier and girder. The target structure was modeled by one DOF model and the entire superstructure is assumed to move rigidly. By inputting observation record at the pier top and setting the parameters such as stiffness and the damping ratio,

we can get the acceleration response of the superstructure. In the next step, the characteristics of the superstructure of Matsunohama Viaduct will be summarized and discussed.

The equation of motion for a one-degree of freedom lumped mass model subjected to earthquake excitation \ddot{z} is calculated by Eq. (2)

$$\ddot{x} + 2h\omega\dot{x} + \omega^2x = -\ddot{z} \quad (2)$$

Where h and ω stand for damping ratio and natural circular frequency respectively. Besides, \ddot{x} , \dot{x} and x stand for displacement, velocity and acceleration of the lumped mass, respectively. Therefore, two parameters, stiffness $K(\equiv m \times \omega_0^2)$ and damping ratio h are subject to be identified.

Owing to its efficiency and simplicity in processing vibration measurements and the lack of requirement for input excitation measurements, the Random Decrement technique (RDT) is applied to evaluate the damping ratio of the structures. In most cases, RDT is applicable to free stationary response data with long duration. Additionally, many approaches to identify damping ratios using the RDT together with Hilbert-Huang transform or Ibrahim time domain technique have been proposed. These approaches⁸⁾⁻¹⁰⁾ state that it is possible to utilize RDT to get damping ratio from earthquake response. In addition, they also show good identification results only based on acceleration records from large earthquakes like El Centro record 1940 Imperial Valley Earthquake. Among these approaches, filtering the noise part from original nonstationary ambient response signal or obtaining the intrinsic mode functions¹¹⁾ are efficient ways. Therefore, the reduced RD signature could perform like true free vibration response. Since collision between the stopper installed in the transverse direction and the superstructure exists¹²⁾, 1DOF system cannot perform the same result in high frequency domain. Therefore, the observation in high frequency domain was considered as the nonstationary ambient response signal. Band pass filter has been applied in this study in the first step and only the frequency wave less than 10Hz remains. In addition, this is also the same setting with the previous study setting⁵⁾ so that we can compare the results with the previous study directly.

In the next step, local maximum of the response acceleration was picked up and overlapped one by one to form an RD wave. During this process, the response acceleration $\ddot{x}(t)$ is indicated by the sum of damped vibration $\dot{D}(t)$ and forced vibration $\dot{R}(t)$. Since $\dot{R}(t)$ is a random waveform, $\sum \dot{R}(t)$ can be offset by overlapping the peaks. On the other hand, $\sum \dot{D}(t)$ becomes larger and forms a RD wave. In this way, the free decay response of the structure is ex-

tracted by the RDT based on this filtered vibration. The envelope function of the damped oscillation waveform can be expressed as Eq. (3)

$$\ddot{x}(t) = \{A \sin(\sqrt{1-h^2}\omega t - \Psi)\}h^2\omega^2 e^{-h\omega t} \quad (3)$$

where the parameters A , ω , h , Ψ stand for the amplitude, frequency, damping ratio and phase difference respectively.^{13),14)} This is the principle of the RDT and the damping ratio can be obtained by this formed logarithmic decreased RD wave by Eq. (4)

$$h = \frac{1}{2\pi} \ln \frac{\ddot{x}_i}{\ddot{x}_{i+1}} \quad (4)$$

In the next step, on the basis of the damping ratio calculated from RDT, the following analysis steps have been used to estimate the stiffness of structures.

- (1) Set the initial stiffness based on designed equation in the Design Manual of Bridge Bearing.
- (2) Get the analyzed acceleration results by the software OPENSEES.
- (3) From the acceleration observation record and the analyzed acceleration results, the value “E” based on the RMS value evaluation function can be calculated as shown in Eq. (5).

$$E = \sqrt{\sum_{t=t_{initial}}^{t_{final}} \frac{\{x(\ddot{t})_{obs} - x(\ddot{t})_{ana}\}^2}{N}} \quad (5)$$

where N stands for total recorded times number. Besides, $x(\ddot{t})_{obs}$ and $x(\ddot{t})_{ana}$ stand for the observed and the analyzed acceleration respectively.

- (4) By increasing the stiffness 1 N/mm² per time, step (2) and (3) were repeated. The identified best fit stiffness is defined as the value that can minimize the RMS value evaluation function.

In addition, the Fourier Spectrum of Girder and the acceleration transfer function between pier top and girder were plotted and discussed. So that we can compare the results with the observation in frequency domain.

5. 1DOF MODEL SEISMIC RESPONSE ANALYSIS ON KOBE EARTHQUAKE

(1) Case1: According to the setting in design manual of bridge bearing

During the 1995 Kobe Earthquake, the objective bridge is located in the region, where JMA Seismic Intensity of 4. Its damping ratio was subject to be identified by RDT. The corresponding free decay response can be formed as shown in Fig.12. So that the damping ratio is 7.8% by Eq. (4). Additionally, its initial stiffness setting was based on the initial

properties of the LRBs installed between pier top and girder in P408 shown in Table 2 and designed equation of calculation in “Design Manual of Bridge Bearing”, its shear modulus and stiffness can be calculated as Eq. (6) and Eq. (8)

$$G(\gamma) = Ge + q(\gamma) \frac{k}{\gamma} \quad (6)$$

$$q(\gamma) = 29.7\gamma \quad (\gamma \leq 0.35) \quad (7)$$

$$K_s = \frac{G(\gamma)A_e}{\sum t_e} \quad (8)$$

In this case, its equivalent shear modulus can be calculated as 2.9 N/mm² when the shear strain is less than 35%. Therefore, its corresponding stiffness is given as 19676.3 N/mm. With this setting, characteristic properties are summarized in Table 3. Based on this setting, the maximum acceleration of the girder is 153.2 gal, the maximum displacement is 51.8 mm and the shear strain is 41.1% in this case. In this case, the corresponding evaluation function result can be calculated as 40.4 gal by Eq. (5). Since the transfer function between pier top and girder represents the frequency characteristics of the seismic base isolated layer, the transfer functions between pier top and girder is calculated and the peak shows at 1.17 s in order to clarify the frequency response of the vibration. In addition, the result of acceleration identification and the transfer functions between pier top and girder are plotted shown in Fig.13.

(2) Case2: According to the previous research

Yoshida et al.⁵⁾ has also done research to evaluate the performance of Matsunohama Viaduct P408 during 1995 Kobe earthquake based on observed records by the model of one degree of freedom system. The corresponding stiffness and damping ratio is given as 47140 N/mm and 13.2% respectively at previous study based on the Bootstrap method. Due to Bootstrap method, the following analysis steps have been used to estimate the damping ratio and the stiffness of structures.

- (1) Calculate the theoretical acceleration transfer function between pier top and girder expressed in form of Eq.(9)

$$H(f) = \frac{f}{-f^2 + 2ih \frac{\omega_0}{2\pi} f + \left(\frac{\omega_0}{2\pi}\right)^2} \quad (9)$$

- (2) Calculate the acceleration transfer function in form of Eq.(10) based on the observation records.

$$\bar{H}(f) = \frac{\sum_{n=1}^N \overline{\ddot{x}_n}(f) \overline{\ddot{z}_n}(f)^*}{\sum_{n=1}^N |\overline{\ddot{z}_n}(f)|^2} \quad (10)$$

Here separate the observed acceleration records into N subsections and find Fourier transform for each section. The Fourier transform are expressed as $\bar{z}_n(f)$ and $\bar{x}_n(f)$. Besides, $\bar{z}_n(f)^*$ is the complex conjugate form of $\bar{z}_n(f)$.

- (3) The evaluation function E was calculated in form of Eq.(11). The identified best fit stiffness and damping ratio are defined as the value that can minimize the evaluation function

$$E = \int \{|H(f)| - |\bar{H}(f)|\}^2 df \quad (11)$$

The maximum acceleration of the girder is 154.6 gal, the maximum displacement is 21.2 mm and the shear strain is 16.8%. The corresponding evaluation function result is 36.5 gal and the peak of the transfer functions between pier top and girder shows at 0.77 s. The result of acceleration identification and the transfer functions between pier top and girder are plotted shown in **Fig.14** and characteristic properties are summarized in **Table 4**.

(3) Case3: Best fit result in this study

Its damping ratio was also subject to be identified by RDT. The corresponding free decay response can be formed as shown in **Fig.12**. So that the damping ratio is 7.8% by Eq. (4). After that, the stiffness was increased 1 N/mm² per time from the Design Manual of Bridge Bearing setting and the corresponding analyzed acceleration results was got by the software OPENSEES. From the acceleration observation record and the analyzed acceleration results, the RMS value evaluation function was calculated. The identified best fit stiffness is defined as the value that can minimize the RMS value evaluation function. By this method, its stiffness was set as 38710 N/mm. With these settings, characteristic properties are summarized in **Table 5**. In this case, the maximum acceleration of the girder is 155.3 gal, the maximum displacement is 25.9 mm and the shear strain is around 20.1%. The corresponding evaluation function result is 33.9 gal and the transfer functions between pier top and girder are calculated and the peak shows at 0.73 s. In addition, the result of acceleration identification and the transfer functions between pier top and girder are plotted as shown in **Fig.15**.

(4) Case4: According to the experiment data

In this case, we can find out that the shear strain is 20.1% based on my best fit result. From the horizontal loading experiment results by Hanshin Expressway as shown in **Fig.5**, we can pick up that the corresponding equivalent stiffness is 37500N /mm and the damping ratio is also set to be 7.8% based on RDT. With this setting, characteristic properties are summarized in **Table 6**. In this case, the maximum

acceleration of the girder is 163.7 gal, the maximum displacement is 25.6 mm and the shear strain is around 20.0%. The corresponding evaluation function result is 37.9 gal and the transfer functions between pier top and girder are calculated and the peak shows at 0.85 s. In addition, the result of acceleration identification and the transfer functions between pier top and girder are plotted shown in **Fig.16**.

(5) Summary

The Fourier spectrum of the girder in case2 and case3 are plotted in **Fig.17**. From the comparison, we can find that the identification result of girder based on both Yoshida et al. research⁵⁾ setting and my best fit result match with the observation records well. Therefore, the RDT together with RMS value evaluation function is feasible and valid. The application by either Bootstrap method or the RDT together with RMS value evaluation function demonstrated their effectiveness.

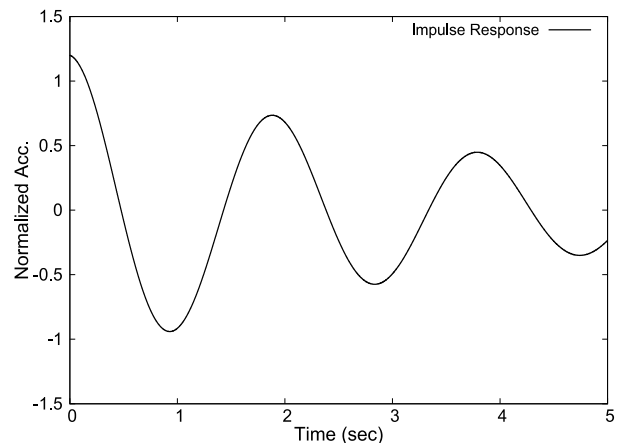


Fig.12 Formed free-decay response by RDT.

Table 2 Initial setting properties of LRBs.

Shear modulus	8	kg/cm ²
Width of the bearing	830	mm
Length of the bearing	1030	mm
Diameter of each plug	120	mm
Numbers of the bearings	4	
Numbers of rubber layers	6	
Thickness of the rubber layer	21	mm

Table 3 The characteristic properties (case 1).

	obs (filtered)	ana(case 1)
Stiffness	19676 N/mm	
Damping ratio	7.8%	
Acc. Max [gal]	135.5	153.2
Disp. Max[mm]	13.2	51.8
Evaluation function RMS Value (E) [gal]	/	
Transfer Function Peak Period [s]	0.73	1.17

Table 4 The characteristic properties (case 2).

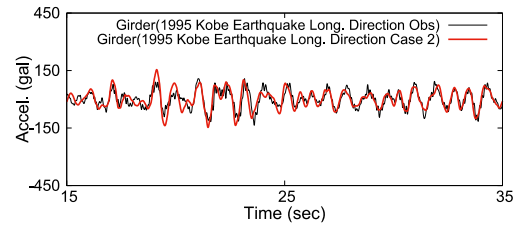
	obs (filtered)	ana(case 2)
Stiffness	47140 N/mm	
Damping ratio	13.2%	
Acc. Max [gal]	135.5	154.6
Disp. Max[mm]	13.2	21.2
Evaluation function	/	
RMS Value (E) [gal]	36.5	
Transfer Function	0.73	0.77
Peak Period [s]		

Table 5 The characteristic properties (case 3).

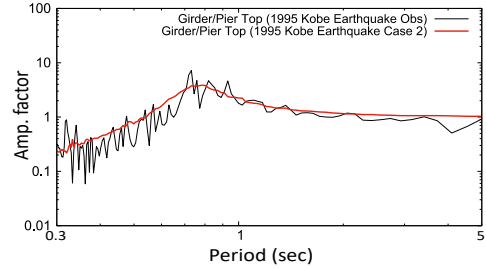
	obs (filtered)	ana(case 3)
Stiffness	38710N/mm	
Damping ratio	7.8%	
Acc. Max [gal]	135.5	155.3
Disp. Max[mm]	13.2	25.9
Evaluation function	/	
RMS Value (E) [gal]	33.9	
Transfer Function	0.73	0.73
Peak Period [s]		

Table 6 The characteristic properties (case 4).

	obs (filtered)	ana(case 4)
Stiffness	37500N/mm	
Damping ratio	7.8%	
Acc. Max [gal]	135.5	163.7
Disp. Max[mm]	13.2	25.6
Evaluation function	/	
RMS Value (E) [gal]	37.9	
Transfer Function	0.73	0.85
Peak Period [s]		

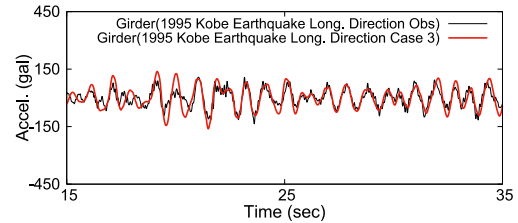


(a) Identification result in long. direction

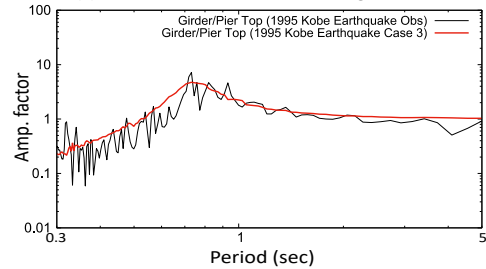


(b) Transfer function in long. direction

Fig.14 Identification result and transfer function (Case2).

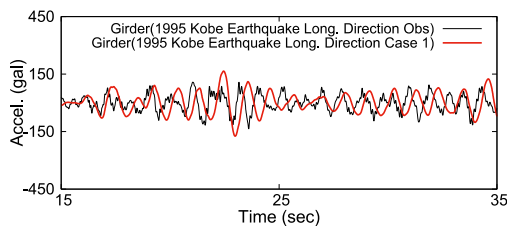


(a) Identification result in long. direction

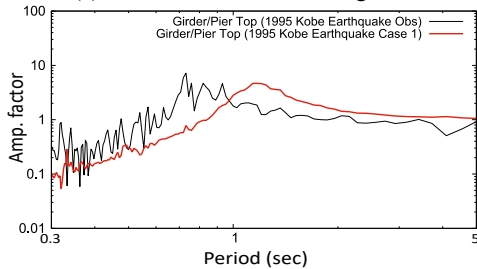


(b) Transfer function in long. direction

Fig.15 Identification result and transfer function (Case3).

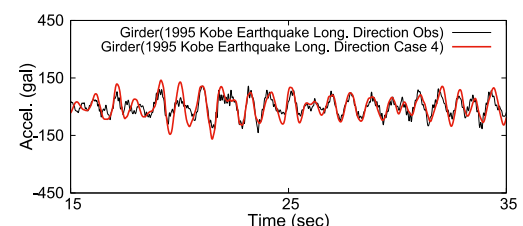


(a) Identification result in long. direction

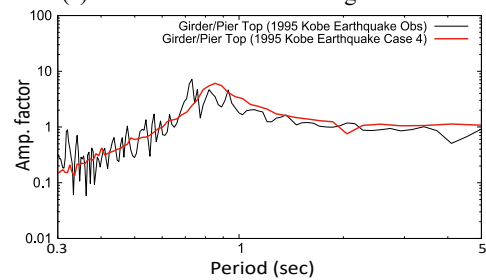


(b) Transfer function in long. direction

Fig.13 Identification result and transfer function (Case1).



(a) Identification result in long. direction



(b) Transfer function in long. direction

Fig.16 Identification result and transfer function (Case4).

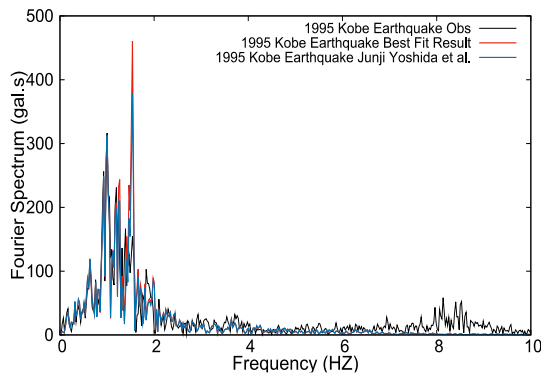


Fig.17 Fourier spectrum of girder (1995 Kobe Earthquake mainshock).

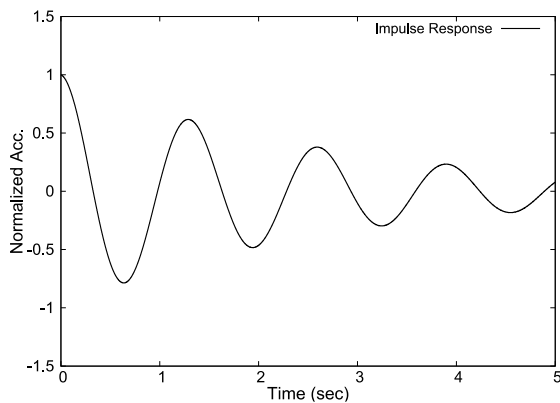


Fig.18 Formed free-decay response by RDT.

Table 7 The characteristic properties (case 1).

	obs (filtered)	ana(case 1)
Stiffness	38710N /mm	
Damping ratio	7.8%	
Acc. Max [gal]	148.0	82.1
Disp. Max[mm]	19.7	13.9
Evaluation function	/	
RMS Value (E) [gal]		
Transfer Function	0.55	0.76
Peak Period [s]		

Table 8 The characteristic properties (case 2).

	obs (filtered)	ana(case 2)
Stiffness	76969N /mm	
Damping ratio	7.7%	
Acc. Max [gal]	148.0	166.6
Disp. Max[mm]	19.7	14.3
Evaluation function	/	
RMS Value (E) [gal]		
Transfer Function	0.55	0.56
Peak Period [s]		

6. 1DOF MODEL SEISMIC RESPONSE ANALYSIS ON OSAKA EARTHQUAKE MAINSHOCK

(1) Case1: Best fit result based on 1995 Kobe EQ

Based on the Best Fit Result setting model from 1995 Kobe Earthquake whose corresponding stiffness and damping ratio are given as 38170 N/mm and 7.8% respectively (case 3 in Chapter 5). In this situation, the maximum acceleration of the girder is 82.1 gal, the maximum displacement is 13.9 mm and the shear strain is 11.0%. The corresponding evaluation function result is 10.8 gal and the peak of the transfer functions between pier top and girder shows at 0.76 s. In addition, the result of acceleration identification and the transfer functions between pier top and girder are plotted shown in **Fig.19** and characteristic properties are summarized in **Table 7**. From the comparison, we can realize that the matching stiffness from previous best fit result is supposed to be smaller than the real situation.

(2) Case2: Best fit result in this study

Its damping ratio was also subject to be identified by RDT. The corresponding free decay response can be formed as shown in **Fig.18**. So that the damping ratio is 7.7% by Eq. (4). After that, the stiffness was increased 1 N/mm² per time from the Design Manual of Bridge Bearing setting and the corresponding analyzed acceleration results was got by the software OPENSEES. From the acceleration observation record and the analyzed acceleration results, the RMS value evaluation function was calculated. The identified best fit stiffness is defined as the value that can minimize the RMS value evaluation function. By this method, its stiffness was set as 76969 N /mm.

With this setting, characteristic properties are summarized in **Table 8**. In this case, the maximum acceleration of the girder is 166.6 gal, the maximum displacement is 14.3 mm and the shear strain is around 11.3%. The corresponding evaluation function result is 9.9 gal and the transfer functions between pier top and girder is calculated and the peak shows at 0.56 s. In addition, the result of acceleration identification and the transfer functions between pier top and girder are plotted shown in **Fig.20**.

(3) Summary

From Fourier spectrum comparison shown in **Fig.21**, it can detected that the identification result of girder based on my best fit result (case2) does match with the observation in frequency domain well compared with previous best fit result (case1) setting in 1995 Kobe Earthquake. From the comparison, we can find that the setting stiffness of the best fit result

in 2018 Osaka Earthquake is around twice larger than that in 1995 Kobe Earthquake. As the maximum acceleration in both earthquakes are in the same range, this difference may be caused by the deterioration of the bearings. Since 23 years have been passed, influence of the deterioration such as aging of the bearings could be possible reasons. This guess matches with previous study result⁴⁾ that the stiffness of the LRBs will increase because of the aging of the LRBs.

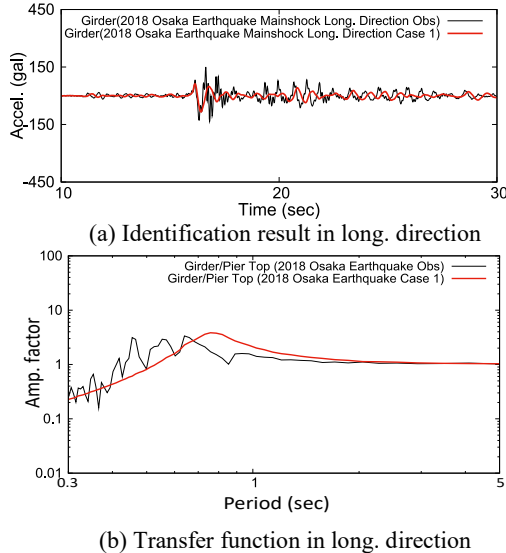


Fig.19 Identification result and transfer function (Case1).

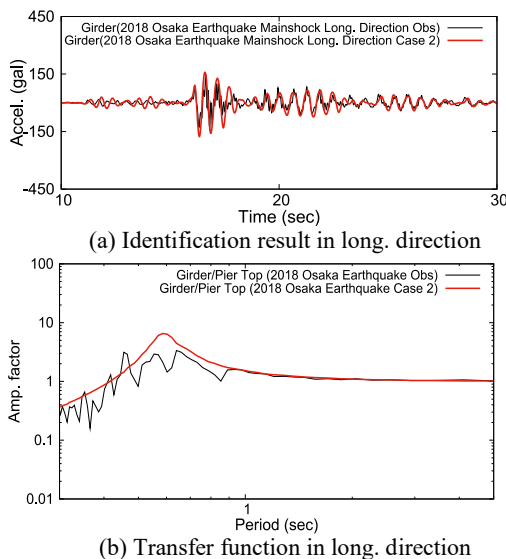


Fig.20 Identification result and transfer function (Case2).

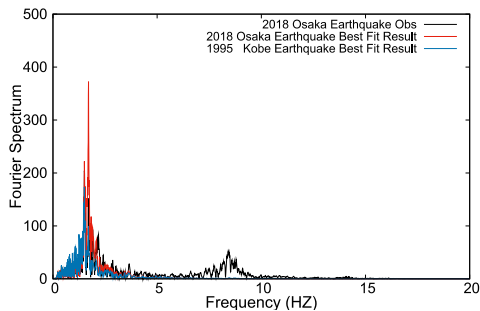


Fig.21 Fourier spectrum of girder (2018 Osaka Earthquake mainshock).

7. 1DOF MODEL SEISMIC RESPONSE ANALYSIS ON OSAKA EARTHQUAKE AFTERSHOCK

(1) Case1: Best fit result based on 2018 Osaka Mainshock Earthquake

The best fit result based on the aftershock of 2018 Osaka Earthquake has also been considered. Based on the best fit result setting in the mainshock of 2018 Osaka Earthquake (case 2 in Chapter 6), the characteristic properties are summarized in **Table 9**. In this case, the maximum acceleration of the girder is 3.8 gal, the maximum displacement is 0.39 mm and the shear strain is around 0.31%. The corresponding evaluation function result is 0.75 gal. The result of acceleration identification is plotted shown in **Fig.22**.

(2) Case2: Best fit result based on 2018 Osaka Aftershock Earthquake

With the same method, the corresponding parameters have also been detected based on RDT and RMS evaluation function. In this case, its stiffness was set as 97275N /mm and the damping ratio is set to 6.1%. With this setting, characteristic properties are summarized in **Table 10**. In this case, the maximum acceleration of the girder is 5.3 gal, the maximum displacement is 0.4 mm and the shear strain is around 0.32%. The corresponding evaluation function result is 0.68 gal. The result of acceleration identification is plotted shown in **Fig.23**.

(3) Summary

The Fourier spectrum of the best fit results during the mainshock and aftershock are plotted in **Fig.24**. Compared with the best fit identification result in the mainshock and the aftershock of 2018 Osaka Earthquake, it can be found that the identified bearing stiffness in aftershock is larger than that in the mainshock. This shows the same result with the previous studies that the stiffness is much larger during the aftershock¹⁵⁾. The influence of the friction in metal bearings is one possible reason and the magnitude of the friction is hard to ascertain precisely because of many uncertainties such as aging and corrosion. Additionally, the damping ratio tends to be smaller than that in the mainshock. The stiffness is larger than that in the mainshock. This also gives the same result as the previous study³⁾.

8. FURTHER DISCUSSION

All the equivalent shear modulus, natural periods, damping ratio and stiffness for best fit results are summarized in **Table 11**. The corresponding best fit equivalent shear modulus has been plotted in **Fig. 25**.

Table 9 The characteristic properties (case 1).

	obs (filtered)	ana(case 1)
Stiffness	76969N /mm	
Damping ratio	7.7%	
Acc. Max [gal]	3.98	3.8
Disp. Max[mm]	0.25	0.39
Evaluation function	/	
RMS Value (E) [gal]		
		0.75

Table 10 The characteristic properties (case 2).

	obs (filtered)	ana(case 2)
Stiffness	97275N /mm	
Damping ratio	6.1%	
Acc. Max [gal]	3.98	5.3
Disp. Max[mm]	0.25	0.40
Evaluation function	/	
RMS Value (E) [gal]		
		0.68

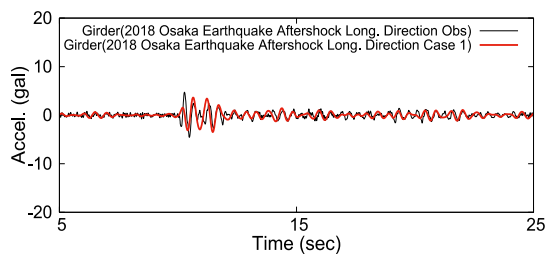


Fig.22 Identification result in long. direction (Case1).

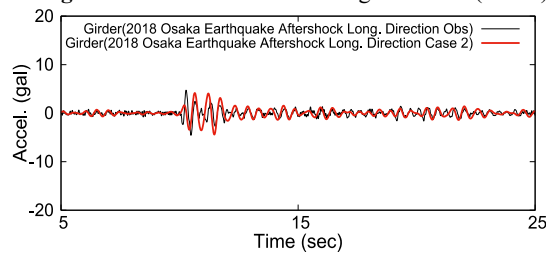


Fig.23 Identification result in long. direction (Case2).

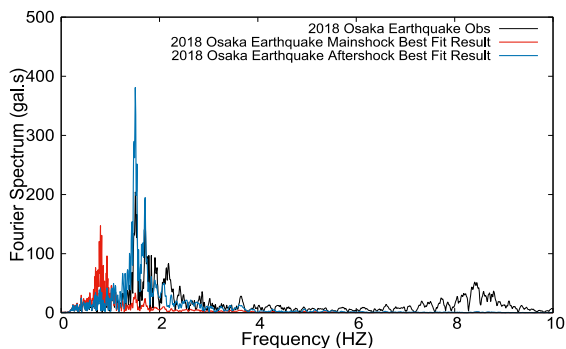


Fig.24 Fourier Spectrum of Girder (2018 Osaka Earthquake Aftershock).

It can be detected that the best fit result equivalent shear modulus and stiffness in 2018 Osaka Earthquake Mainshock is 1.99 times that of the previous best fit result in 1995 Kobe Earthquake. And the best fit result natural frequency in 2018 Osaka Earthquake Mainshock is 1.26 times that in 1995 Kobe Earthquake. The objective bridge is located in the region, where JMA Seismic Intensity of 4 in both earthquakes and the maximum acceleration in both earthquake are also in the same range. Therefore, this discrepancy may be attributed to the deterioration of the bearings. Since 23 years have been passed, influence of the deterioration such as aging and humidity of the bearings could have huge effect.

Besides, final calculated damping ratios of the lead rubber bearing in this study are 7.8%, 7.7% and 6.1% in longitude direction based on RDT for 1995 Kobe Earthquake, mainshock and aftershock of the 2018 Osaka Earthquake. From the experiment results, it shows that the corresponding damping ratio should be 7.3% when the displacement is 12.5mm.⁷⁾ We can see that the damping ratio results calculated by the RDT show a similar result with the experiment results. However, it needs to be pointed out that either in very small shear strain region or large scale earthquake situation, filters such as low pass filter and band pass filter needs to be used. Otherwise, too much noise or other vibration components could be mixed into the RD waveform so that the damping ratio will be miss estimated.

Table 11 Best fit result characteristic properties.

	1995 Kobe EQ Mainshock
Equivalent shear modulus	5.2 N/mm ²
Natural Frquency	1.233 Hz
Damping Ratio	7.8%
Stiffness	38710N /mm

	2018 Osaka EQ Mainshock
Equivalent shear modulus	10.3 N/mm ²
Natural Frquency	1.738 Hz
Damping Ratio	7.7%
Stiffness	76969N /mm

	2018 Osaka EQ Aftershock
Equivalent shear modulus	13.1 N/mm ²
Natural Frquency	1.957 Hz
Damping Ratio	6.1%
Stiffness	97275N /mm

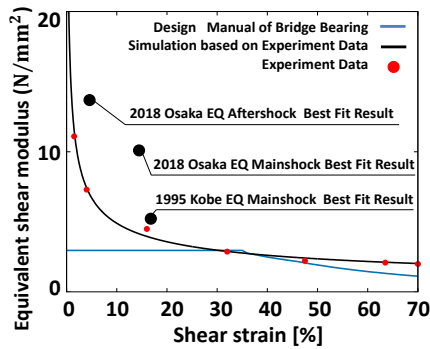


Fig.25 Relationship between shear strain and equivalent shear modulus.

9. CONCLUSION

Based on the seismic response analysis on Matsunohama Viaduct using system identification method and the evaluations on the stiffness and damping ratio during both the 2018 Osaka Earthquake as well as the 1995 Kobe Earthquake, following conclusions have been drawn:

- (1) Combinations of the RDT and evaluation function based on the RMS value calculation have been used to identify the structural parameters. Additionally, the application demonstrated its effectiveness.
- (2) From the comparison, it can be found that the natural frequency changed from 1.233 Hz to 1.738 Hz and the equivalent shear modulus changed from 5.2 N/mm² to 10.3N/mm², which is 1.99 times that of the previous best fit result. Although the equivalent stiffness tends to increase since the deformation in 2018 Osaka Earthquake is slightly smaller, it is also reasonable to claim that the stiffness is larger than the expected value from the comparison.
- (3) The discrepancy between the identification result stiffness in 1995 Kobe Earthquake and 2018 Osaka Earthquake may be attributed to the deterioration of the bearings like aging.
- (4) Although this study was focused on the slightly strong earthquakes, it should be very useful result for future study to find the effective relation between the isolators performance during the large scale earthquake and slightly strong earthquake. In addition, experiment test are also expected to be done to find the corresponding with high precision. Therefore we can enhance the seismic performance of structures before real large scale earthquake occurs.

ACKNOWLEDGMENT: The authors would like to thank Hanshin Expressway Corporation, Hanshin Expressway Technology Center and National Institute for Land and Infrastructure Management, MLIT for sharing the observation records and information of our target viaducts.

REFERENCES

- 1) Toshiro, H. and Felix, D. R. J.: Effect of hardening of lead rubber bearings on nonlinear behavior of highway viaduct under great earthquake, *13th World Conference on Earthquake Engineering Vancouver*, B. C., Canada August 1-6, 2004, Paper No. 3332, 2004.
- 2) Eem, S. and Daegi, H.: Large strain nonlinear model of lead rubber bearings for design basis earthquakes, *Nuclear Engineering and Technology*, Vol. 51, pp. 600-606, 2019.
- 3) Sugiyama, Y., Toyoshima, M., Chiba, D. and Kurita, S.: Characteristics of nonlinear restoring forces of base-isolation devices at small strains based on seismic response records, Part 3 - Lead rubber bearing, *J. Struct. Constr. Eng. AIJ*, No. 587, pp. 85-92, Jan. 2005.
- 4) Dang, J., Higashide, T., Igarashi, A., Adachi, Y. and Hayashi, T.: Dynamic analysis to investigate the effect of aging deterioration of lead rubber bearings on the seismic performance of bridges, *Japan Society of Civil Engineers, Structural Engineering and Earthquake Engineering*, Vol. 71, No. 4, pp. 713-724, 2015. (in Japanese)
- 5) Yoshida, J., Abe, M. and Fujino, Y.: Performance of base-isolated bridge during 1995 Kobe Earthquake based on observed records, *Proc. JSCE*, No. 626/I-48, pp. 27-50, 1999.
- 6) Kiyono, J.: Report on the damage surveys and investigations following the 2018 Hokkaido Iburi Tobu & Northern Osaka Earthquake, *Japan Society of Civil Engineers*, pp. 1-22, 2019. (in Japanese)
- 7) Horimatsu, M., Komatsu, I., Sasaki, N. and Nakaya, S.: Vibration experiments and dynamics response analysis using the actual highway bridge with base isolators, *The Bridge and Foundation Engineering*, Vol. 94, No. 4, pp 25-32, 1994. (in Japanese)
- 8) Rodrigues, J. and Brincker, R.: Application of the random decrement technique, *Proc. 1st International Operational Modal Analysis Conference*, Iomac, 2005.
- 9) Yukawa, M., Shingu, K. and Hiratsuka, K.: Comparison on damping ratios of an earthquake proof structure, a seismic strengthening structure and a base isolated retrofit structure, *Theoretical and Applied Mechanics Japan, Dynamics and Optimization*, Vol. 56, pp. 143-152, 2008.
- 10) Lin, C. C., Hong, L. L., Ueng, J. M., Wu, K. C. and Wang, C. E.: Parameter identification of asymmetric building from earthquake response records, *Smart Mater. Struct.*, Vol. 14, 2005.
- 11) Han, J. P., Li, L., Wang, H. T. and Qian, J.: Modal parameter identification based on Hilbert-Huang transform and random decrement technique, *World Earthquake Engineering*, Vol. 27, No. 1, Mar. 2011. (in Chinese)
- 12) Kono, T. and Kawashima, K.: Vibration characteristics of base isolated bridges based on measured strong motion records, *24th Proc. JSCE*, pp. 329-332, Jul. 1997. (in Japanese)
- 13) Tamura, Y., Sasaki, A. and Tsukagoshi, H.: Evaluation of damping ratios of randomly excited buildings using the Random Decrement Technique, *J. Struct. Constr. Eng. AIJ*, No. 454, pp. 29-38, Dec. 1993. (in Japanese)
- 14) Toyoda, T. and Takano, K.: Estimating the damping ratio of buildings using weak seismic ground motion: A case study on buildings of the University of Tokyo, *Bull. Earthq. Res. Inst. Univ. Tokyo*, Vol. 88, pp. 1-36, 2013. (in Japanese)
- 15) Chaudhary, M. T. A., Abe, M., Fujino, Y. and Yoshida, J.: System Identification of two base-isolated bridges using seismic records, *J. Struct. Eng.*, Vol. 126, No. 10, pp. 1187-1195, 2000.

(2019.11.12 Received, 2020.1.31 Revised, 2020.2.16 Accepted)